Research Open

Geology, Earth and Marine Sciences
Volume 3 Issue 3

Research Article

Fluid Inclusions and Metallogenic Conditions of the Dashuigou Tellurium Deposit, Tibet Plateau, Southwest China

Jianzhao Yin[1]* and Hongyun Shi[2]

[1]Ph.D., Orient Resources Ltd., Richmond, British Columbia, Canada V7E 1M8
[2]Ph.D., Bureau Veritas Commodities Canada Ltd., Richmond, BC, Canada V7A 4V5

Corresponding author: Jianzhao Yin, Ph.D, Orient Resources Ltd., Richmond, British Columbia, Canada V7E 1M8; **Tel:** 1-778-668.7717; **Email:** jimyin7@yahoo.ca

Received: May 11, 2021; **Accepted:** May 19, 2021; **Published:** May 27, 2021

Abstract

By thoroughly researching the microscopic characteristics and compositions of fluid inclusions in various minerals of the Dashuigou independent tellurium deposit in Southwest China, the authors of this paper uncover metallogenic conditions of the only independent tellurium deposit in the world. The principal compositions of the metallogenic hydrothermal fluids are Na^+, K^+, Ca^{2+}, Mg^{2+}, SO_4^{2-}, Cl^-, F^-, H_2O, CO_2, CH_4, H_2, N_2, CO and C_2H_6. The salinity of fluid inclusions within the metallogenic epochs varies between 13.8%-36.2%, which falls into a medium-high salinity range. The salinity of quartz samples associated with tellurides formed during the tellurium epoch is 14.9%-18.7%, which is within the medium salinity range. Metallogenic pressure is calculated at 0.647-1.020 Kbar, and the corresponding mineralization depth is 4.08-2.16 km. Mineralization temperatures of the deposit's early and late metallogenic epochs are respectively 336.0-406.0 and 216.9-229.0°C. The metallogenic hydrothermal solutions are SO_4^{2-} - Ca^{2+} type, or SO_4^{2-} - Na^+ - K^+ - Ca^{2+} type, especially during the early Pyritic Epoch, and Na^+-K^+-Cl^--SO_4^{2-} type during the late metallogenic epoch. The metallogenic hydrothermal solutions of the deposit are of moderate salinity, mesothermal and mesogenetic.

Keywords: *Metallogenic condition; Fluid inclusion; Homogenization temperature; Decrepitation temperature; Metallogenic epoch; The Dashuigou tellurium deposit; Tibet Plateau*

Introduction

Tellurium (Te) is usually categorized as a scattered or dispersed element (abbreviated as SM). SM are those metals, semimetals and/or nonmetals that have similar geochemical characteristics with Clark values too low to enrich into independent deposits, but that play very important roles in modern science, industry, national defense and at the frontiers of technology. It is thought in the traditional theory of mineral deposits and geochemistry that Te could not form independent deposits, but only exist as associated components in other metallic deposits. The abundance of Te in the Earth's Crust is very low. According to Li [1], the average content of Te in the Earth's crust is 2.0 x 10^{-8} in China, and only 1.34 x 10^{-9} worldwide. At present, the world's supply of refined tellurium is mainly recovered from Te-bearing minerals including pyrite, sphalerite, chalcopyrite, galena, pyrrhotite, volcanogenetic sulfur, bismuthinite, arsenopyrite, and cassiterite, etc. Generally speaking, only sulfide ores containing more than 0.002% Te can be used. As a result, the amount of refined tellurium that can be recovered is very limited. Most of the recoverable Te in the world is from copper deposits, and it is estimated that only 0.065 kg of Te can be produced in the refining process of one ton of copper [2,3]. The Dashuigou tellurium deposit is the only independent tellurium deposit in the world. Since its discovery in 1992, it has aroused widespread concern from domestic geologists. Chen [4] believed that tellurium mineralization is related to Yanshanian alkaline intrusive rocks, while Luo [5,6] believed that the mineralization is related to Yanshanian granitic magma activity. Yin [3,7,8] proposed that scattered elements including tellurium and bismuth originated from gas blown off from the deep Earth and enriched through nano-effect. Wang [9] summarized the metallogenic process of the Dashuigou tellurium deposit as follows: a volcanic eruption deposit was formed on the ancient seafloor with magmatic eruption in the late Proterozoic. Then, the deposit was strongly superimposed and reconstructed by the Mesozoic multistage regional metamorphic hydrothermal activities.

Regional Geology

The Dashuigou tellurium deposit is located in the transitional belt between the Yangtze Platform and Songpan-Ganzi folded belt, as part of the Tibetan Plateau (Figure 1). The deposit is nestled in the convergence between the Indian, Eurasian and Pacific Plates. The crust-mantle structures and properties in the region are the result of tectogenesis through various geological times. It implies the turning boundary of the Earth's crust's thickness. It is also a gravity gradient zone which controls not only the production and development of earthquakes and tectonomagmatic events, but also the distribution of a series of mineral deposits. Geophysical data indicates that the upper mantle below the region uplifts obviously. As a result, the area possesses high heat flow geophysical characteristics [3,5,6,10,11].

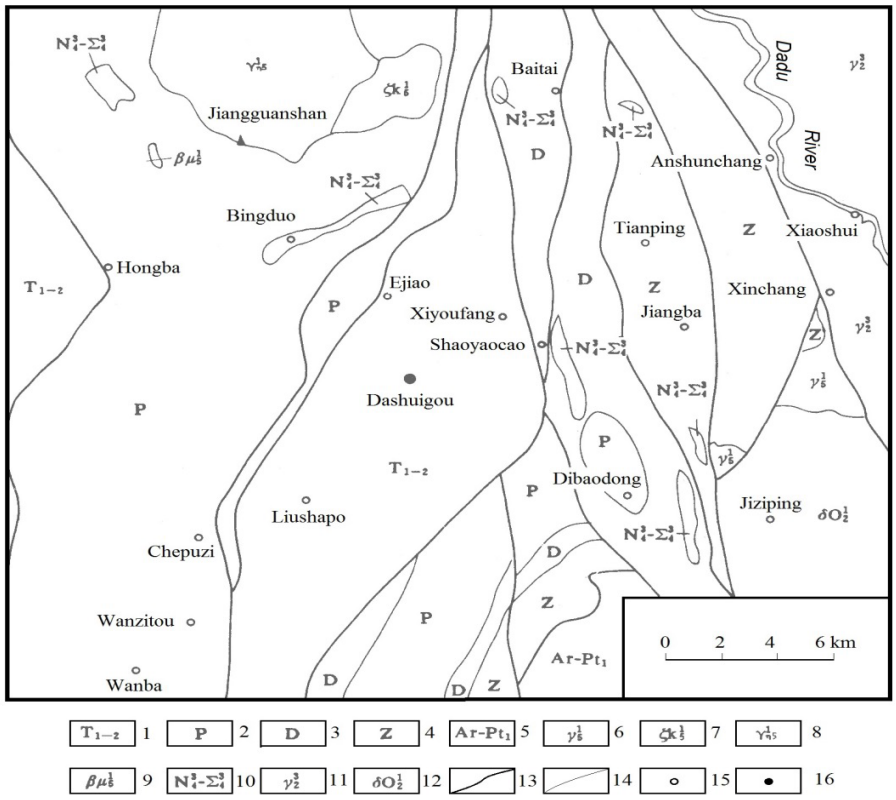

Figure 1: Regional geology (after Yin, 1996).

1. The lower and middle Triassic metamorphic rocks; 2. The Permian metamorphic rocks; 3. The Devonian metamorphic rocks; 4. Metamorphic rocks of the Sinian system; 5. Metamorphic base complex of the Archean Kangding group; 6. Plutonic granite of the Indosinian orogeny; 7. Plutonic alkaline syenite of the Indosinian orogeny; 8. Plutonic monzonitic granite of the Indosinian orogeny; 9. Hypabyssal sillite of the Indosinian orogeny; 10. The late Hercynian basic-ultrabasic rocks; 11. The late Proterozoic plutonic granite; 12. The early Proterozoic-Archean plutonic quartz diorite; 13. The deep and large fault; 14. The geological boundary; 15. Village and/or town; 16. The tellurium deposit. There is also a low-velocity, low resistivity zone in the middle crust that is interpreted as a decollement. The abnormal mantle exists under the crust in the region. It has properties of both geosyncline and platform, as well as its own special characteristics. The belt is a geo-tectonically active zone with very complicated igneous rock structures. According to the regional geophysical data, the region's characteristics exhibit high velocity, high density, high resistance, high geothermal flow, high magnetism as well as well-developed earthquakes and mantle's uplift. In summary, this region is both geologically very active and a very important south-north trending tectonomagmatic-mineral belt [3-6]. The strata, igneous rocks and structures trend south-northward. The strata are low-grade metamorphic rocks of the Silurian, Devonian, Permian systems and middle-lower Triassic series. A large amount of Archaean metamorphic rocks of the Kangding Group emerge to the southeast of the deposit. The well-developed igneous rocks in the region include ultrabasic, basic, neutral, acid and alkaline, produced in different geological times. Different types of mineral resources in the region are very rich; many of these are well known, including Ti, V, Cu, Pb, Zn, SM, REE, coal, asbestos and the Panzhihua Vanadium Titano-magnetite deposit [3-6].

Mine Geology

The strata of the area are low-grade metamorphic rocks of the lower-middle Triassic age, including marble, slate and schist. The main wall-rocks of the ore bodies are schist and slate. All of the Triassic strata make up a NNE-trending dome. The geological and geochemical characteristics in the area indicate that the protolith of the tellurium ore veins' direct wall-rocks is poorly differentiated mantle-derived basalt (Figure 2).

Both faults and folds are well-developed in the area. The annular and linear structures together make up special "Ø" pattern structures, which control the formation of different types of endogenetic mineral deposits, including the Dashuigou tellurium deposit. No intrusive rocks emerge within a 5 km radius around the deposit. Only two small Permian ultrabasic-basic rock bodies emerge within a 10 km range of the deposit. Large neutral, acid and alkaline intrusive bodies exist beyond 10 km, which are unrelated to the deposit (Figure 1). Quantitative chemical analyses of Te, Bi, Se, As, Au, Ag, Cu, Pb and Zn were conducted on different rock samples including granites, metamorphic rocks, altered rocks, and carbonate veins of different geological times. The main findings are summarized below [3,12-15]. The Te content in the granites is under 1 x 10^{-7}, which is similar to its Clark value in the Earth's crust. Te in the metamorphic rocks is slightly higher than in the granites and varies slightly

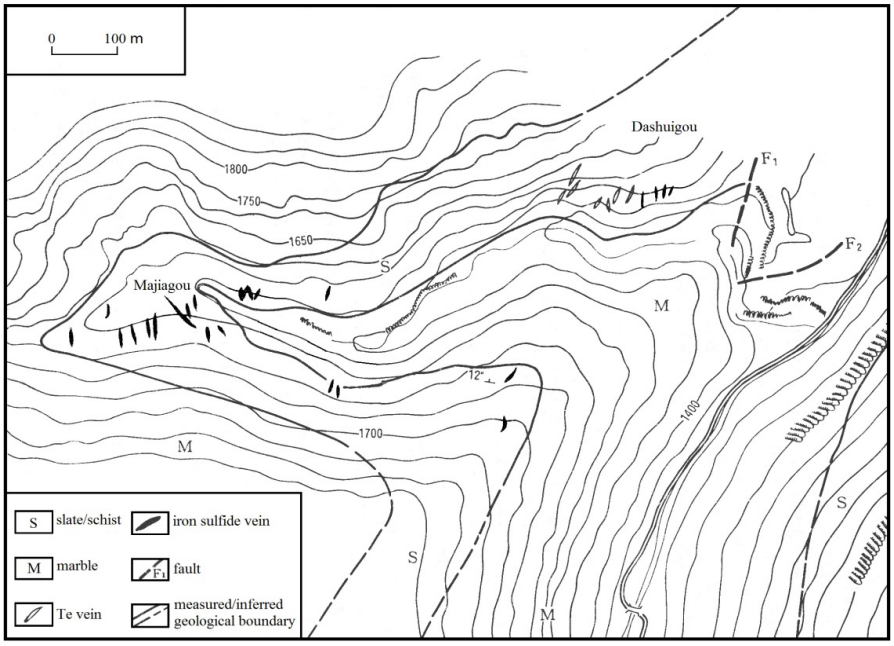

Figure 2: Mine geology (after Yin, 1996).

between metamorphic rocks of different geological times, while being relatively higher in the Triassic metamorphic rocks. Of the metamorphic rocks in the same geological time, the Te content in the slate and schist is higher than in the marble. Te content in rocks of the same stratohorizon of the same geological time also varies; namely, it is higher in rocks within the mining area than in those beyond the mining area. Te content is closely related to the intensity of alterations; that is, the ore-forming elements are not derived from the country rocks, but instead from the mantle. The deposit is located at the northeastern end of the Triassic metamorphic dome. The ore bodies are controlled by and fill a group of shear fractures. Ten tellurium ore veins have been discovered, which strike from 350 to 10 degrees and dip at 55 to 70 degrees westward. Widths of the ore bodies vary between 25 and 30 cm. The narrow ore bodies are in the shape of lenticular veins and have sharp contact with the wall rocks (Figures 3 and 4).

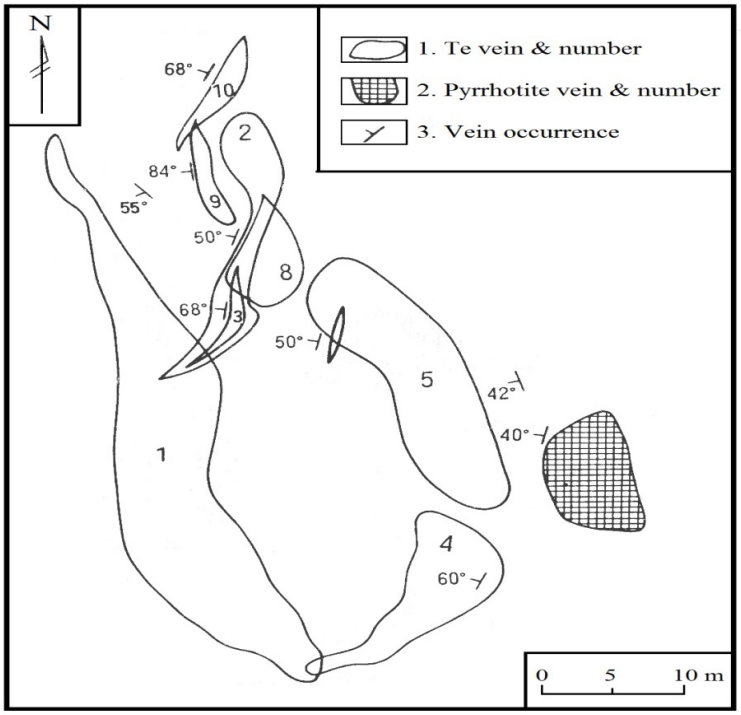

Figure 3: Horizontal projection of the telluride veins of the Dashuigou deposit (after Yin, 1996).

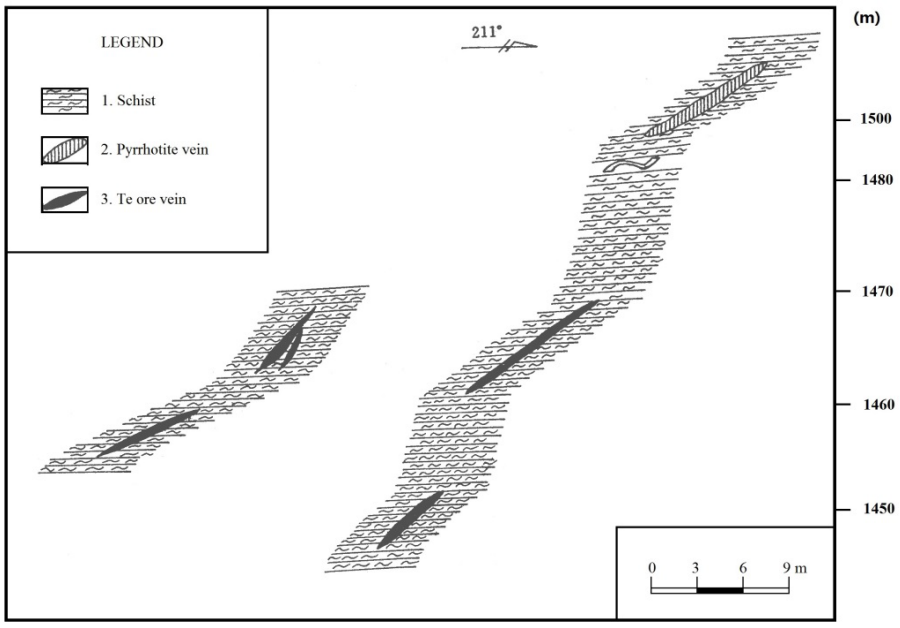

Figure 4: Longitudinal section the telluride and pyrrhotite veins of the Dashuigou deposit (after Yin, 1996).

The altered rocks occur in narrow bands ranging between several centimeters and one meter in thickness. Altered zones beside the massive ore veins are narrower, at only several centimeters wide. The dominant alterations include dolomitization, silicification, biotitization, muscovitizaion, tourmalinization, sericitizaion, greisenization, and chloritization [3,7,14-20]. Approximately thirty minerals are identified in the ore, which include tetradymite, pyrrhotite, pyrite, dolomite, quartz, chalcopyrite, tsumoite (BiTe), tellurobismuthite (Bi_2Te_3), galena, magnetite, gold, silver, electrum, ilmenite, calcite, calaverite, siderite, mannesite, rutile, muscovite, biotite, sericite, hornblende, chlorite, plagioclase, K-feldspar, tourmaline, hematite, garnet, apatite, and epidote. The first five minerals are the most important and comprise 85% of the ore, though generally tetradymite is so rare that many monographs on mineralogy do not have any related data on it [3,10,19-22]. Replacement, remnant, reaction border, and granular are the dominating textures of the ore. Massive, vein/veinlet, stockwork veins are the dominating structures of the deposit (Figures 5 and 6).

The most important ores are massive and the secondary ores are disseminated. The Te content in the ore varies between 0.01% and 34.58%.

Two mineralization epochs and five stages exist in the deposit [3,8,23]:

- Pyrrhotite epoch (177.7~165.1 Ma): including three mineralization stages: carbonate stage (I) → pyrrhotite stage (II) → chalcopyrite stage (III) (from early to late).
- Tellurium epoch (91.71~80.19 Ma): including two mineralization stages, namely: tetradymite stage (I) → tsumoite ($BiTe_{0.97}$) stage (II).

Mineralization Epoch and Mineral Sequence

Based on the mutually crosscutting relationships of various veins/veinlets in the deposit, including those of pyrrhotite, chalcopyrite, tetradymite, tsumoite, dolomite and quartz, in addition to the features of microscopic texture and structure between gangue and ore minerals, the mineralization epochs and stages as well as mineral sequence are summarized in Figure 7 [3,8,23].

Carbonate Stage

A large quantity of iron-dolomite, quartz and lesser calcite veins/veinlets occurred within this stage, which are brown and/or yellowish brown broken coarse-grained due to iron staining (Figures 5 and 6). Decrepitation temperatures of the fluid inclusions in the dolomite, one of the dominant minerals of this stage, are listed in the corresponding table of this paper.

Pyrrhotite Stage

The largest quantity of pyrrhotite formed during this stage. Some coarse- to very coarse-grained pentagonal pyrite can be seen in the anhedral crystals of pyrrhotite. Decrepitation temperatures of the fluid inclusions in both the pyrrhotite, one of the dominant minerals, and pyrite of this stage are listed in the corresponding table of this paper.

Chalcopyrite Stage

Many chalcopyrite veins/veinlets formed within this stage, filling in fractures of pyrrhotite and/or crosscutting pyrrhotite. Part of the chalcopyrite is within telluride minerals in the vermicular form. Decrepitation temperatures of the fluid inclusions in the chalcopyrite, the dominant mineral of this stage, are listed in the corresponding table of this paper.

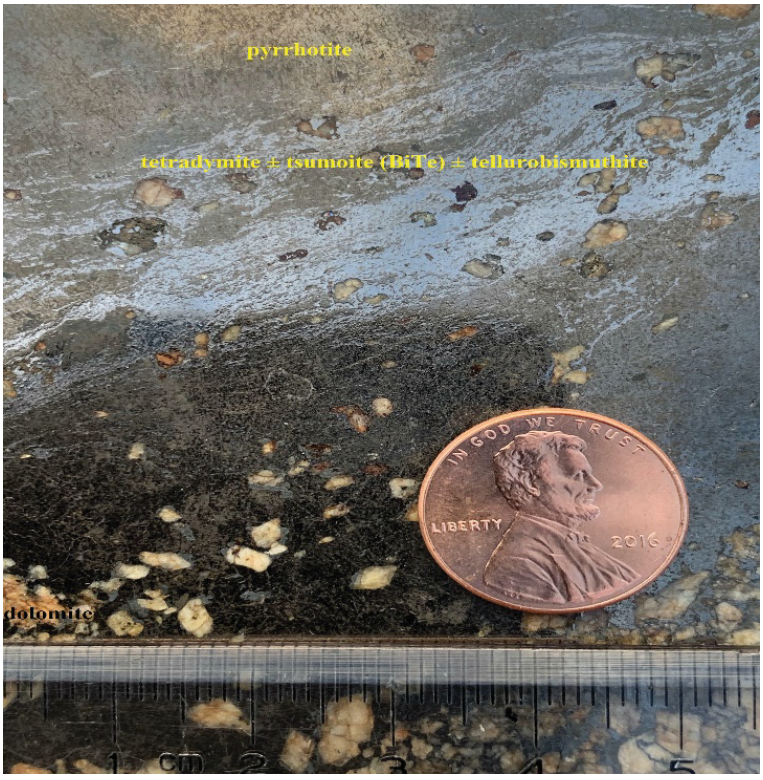

Figure 5: Lead grey-silvery colored tetradymite ± tsumoite (BiTe) ± tellurobismuthite (Bi_2Te_3) fine veinlets in massive pyrrhotite (dark colored background) + dolomite (brownish white) from the deposit (sample #: SD40, Ore body #I-1 in Drift 3).

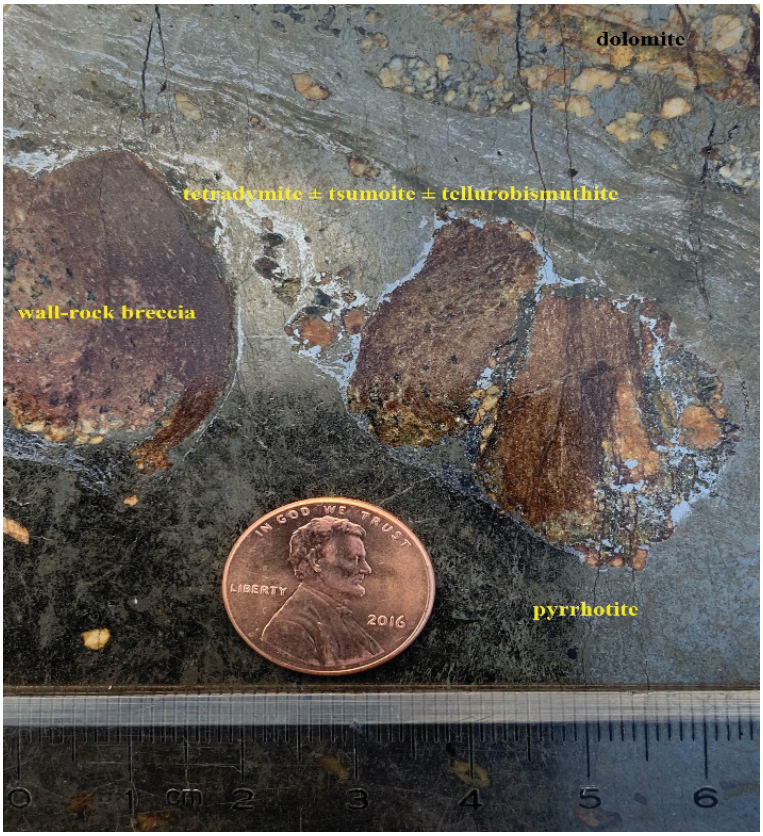

Figure 6: Lead grey-silvery colored tetradymite ± tsumoite (BiTe) ± tellurobismuthite (Bi_2Te_3) fine veinlets in massive pyrrhotite (dark colored) + dolomite (brownish white) + wall rock (dark brown) from the deposit (sample #: SD34, Ore body #I-1 in Drift 3).

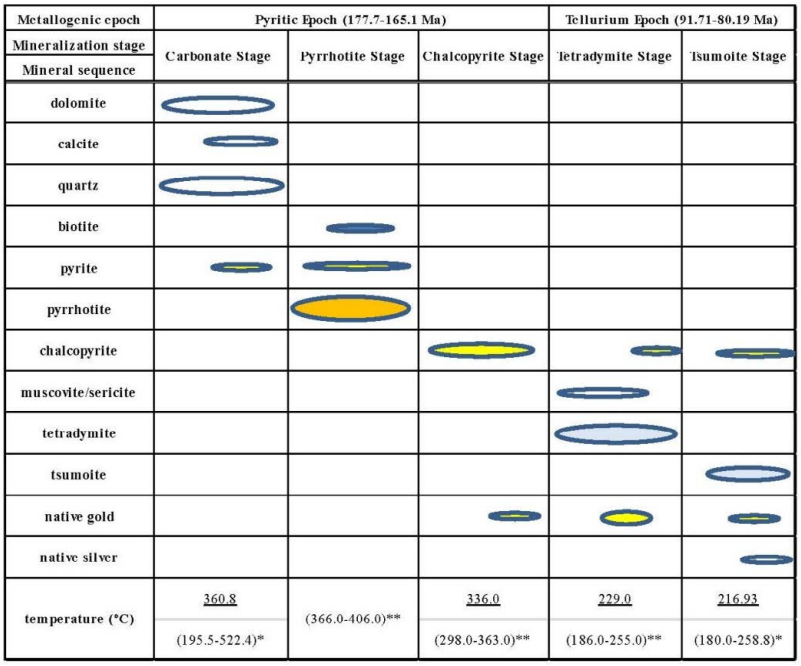

Figure 7: Mineralization epochs & stages and mineral sequence of the deposit.
Note: * - mineral inclusion homogenization temperature (dolomite for carbonate stage, quartz for tsumoite stage), please refer to Tables 1 and 2 for more detailed information; ** - mineral inclusion decrepitation temperatures of the corresponding stages (that of the pyrrhotite stage is the average of decrepitation temperatures of both the pyrite and pyrrhotite of the pyrrhotite stage.

The three prior mineralization stages consist of the early metallogenic epoch of the deposit, the pyritic epoch (177.7-165.1 Ma) of the early Yanshan orogeny. The following two mineralization stages consist of the tellurium metallogenic epoch (91.71-80.19 Ma) of the late Yanshan orogeny [3,24].

Telluride Stage

Large quantities of massive/semi-massive telluride veins formed during this stage, associated with clean, milky-white quartz, dolomite, calcite, muscovite/sericite and native gold. Decrepitation temperatures of the fluid inclusions in the tetradymite, the dominant mineral, and part of the associated dolomite of this stage are listed in the corresponding table of this paper.

Tsumoite Stage

Tsumoite and chalcopyrite together consist of emulsion droplets and/or vermicular immixing of solid solution texture at the contacts between tetradymite and pyrrhotite (Figures 5, 6 and 8).

The mineralization temperatures of this stage shown in Figure 7 are based on the homogenization temperatures of the fluid inclusions in the quartz associated with tsumoite. Please refer to the corresponding table of this paper for more detailed information.

Sampling and Analytical Methodology

Field Sampling

Samples were collected from proper locations of the deposit's typical ore bodies and wall rocks in the study area. They were described in detail on site, then properly labeled or numbered and wrapped with waxed paper to avoid cross contamination with other samples in the same sample box, and finally packed and shipped to the work laboratory.

Lab Sampling and Preliminary Processing

In the lab, all samples were sorted, air-dried, stage crushed to 6-Tyler mesh, well homogenized, and then rotary split into 1 kg assay aliquots. One assay aliquot was wet screened into different sized fractions, and the -10 mesh+65 mesh fraction was used for this study. After being crushed and screened through different sizes of mesh, the corresponding minerals in fraction from 10 to 65 mesh to be used for further analyses were then manually separated and picked up under binocular microscope, and their crystal forms and other physical mineralogical characteristics were observed and described in detail. Next, the selected mineral samples were pulverized to 90% passing 75 μm for further research and testing, in order to help reveal the mineralization mechanism of the corresponding deposit.

Analytical Methodology

The gaseous components of the fluid inclusions in quartz were analyzed via both the Raman spectroscopy and gas chromatographic methods. The Raman spectroscopy technique has a wide field of applications, ranging from qualitative detection of solid, liquid and gaseous components to identification of polyatomic ions in solution. It is also a versatile non-destructive technique for fluid inclusion analysis and is commonly used to calculate the density of CO_2 fluids, the chemistry of aqueous fluids, and the molar proportions of gaseous mixtures present as inclusions... The main advantages of this technique are the minimal sample preparation required and its high versatility. The particle size of the 99.9% purity mineral samples was controlled to 0.5-1.0 mm to avoid damaging the fluid inclusions. According to

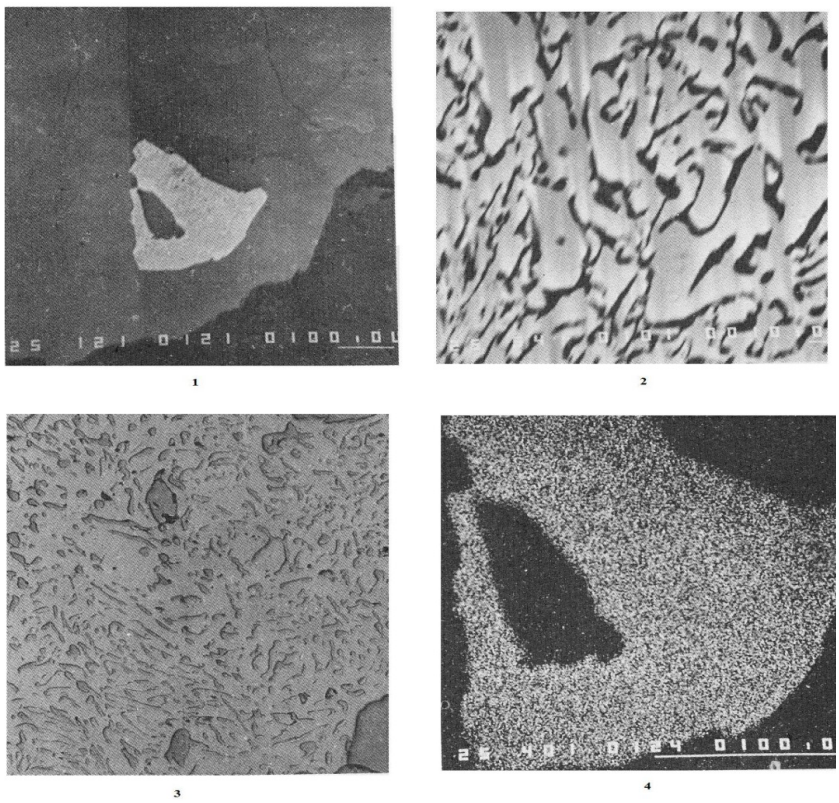

Figure 8: 1~3: Reflection color and their mutual relationships between tsumoite (bright white), tetradymite (white), and pyrrhotite (grey) in the back scattered electron (composition) image from the deposit (thin section (-) (Note: 1 (×120), 2 (×540), & 3 (×200)). 4: Te Kα X ray image indicating chemical composition distributions of telluride including tetradymite and tsumoite (white): the denser the white spots, the higher the Te content; the black colored background is pyrrhotite from the deposit (×400).

their respective burst temperatures, the primary inclusions in the minerals were opened by thermal explosion, and the fluid components obtained by heat-blast-leaching. The released gas-phase components such as H_2O, CO_2, CO, H_2, N_2, and CH_4 were measured by gas chromatography. Decrepitated mineral was added with deionized water, and ultrasonic extraction was then conducted. The extract liquor was measured by atomic absorption spectrometer for K^+, Na^+, Ca^{2+}, Mg^{2+} and other cationic components in the solution, while anion components such as F^-, Cl^-, SO_4^{2-}, etc. were determined through ion chromatography or spectrophotometry. In addition, Fe, Cu, Pb, Zn, Sb, Hg, Au, Ag and other related ore-forming metal elements can be determined by the atomic absorption flameless method as required. Then, the gas and liquid phase components in the mineral inclusions were converted into the mass concentration of each component contained in the mineral inclusion aqueous solution. Conversion of liquid components: At room temperature, 1 ml of water weighs about 1 gram. First, the mass of water in the analysis result is converted into the volume V_{H2O}, and the mass concentration ρ_B of each ion in the inclusion water is calculated via the following formula [25,26]:

The volume of inclusion water $V_{H2O} = \omega_{H2O}/1000$. Mass concentration of ions in liter of water $\rho_B = \omega_B/V_{H2O}$.

For the measurement data of vapor phase components H_2O, CO_2, CO, H_2, and CH_4, a relevant diagram [27] was applied to estimate the temperature, pressure, oxygen fugacity, carbon dioxide fugacity, reduction coefficient, and other geochemical parameters such as pH and Eh of the equilibrium among the components in the mineral inclusions.

Characteristics of the Fluid Inclusions

General Characteristics

The fluid inclusion characteristics of part of the deposit's gangue and ore minerals are summarized in Tables 2 and 3 and discussed as follows. Fluid inclusions are well developed in most of the deposit's minerals, but their characteristics differ from each other within different host minerals. Dolomite usually has less liquid inclusions than both calcite and quartz. The sizes of fluid inclusions in dolomite and calcite are usually between 3-5 μm, which is smaller than those in quartz, which is usually 5-10 μm (Table 2). Fluid inclusions in both dolomite and calcite are mainly liquid and usually scattered without any orientation in mineral distribution, with a gas-liquid ratio of less than 5%. Those in quartz, which are mainly gaseous-liquid inclusions within the deposit, are more complicated than those in both dolomite and quartz; either scattered without any orientation in distribution, or in zonal distribution in certain orientations (Figure 6). Fluid inclusions in the tourmaline-quartz vein collected from the periphery of the deposit are mainly gaseous-liquid inclusions and differ from those of quartz within the deposit; a few 3 phase inclusions could be seen in the quartz vein collected around the deposit.

Table 1 : Decrepitation temperatures of fluid inclusion in the minerals from the deposit.

series #	sample #	mineral	location	test results (°C)		
				principal value	reference value	average
1	SD-10	pyrrhotite	Pyr vein between # II & III Ore Zones	387	64	
2	SD-15		Pyr vein of # III Ore Zone	325	125	
3	SD-16		#III-2 Pyr vein	423	n/a	
4	SD-23		Pyr vein within # I-4 Ore Vein	447	n/a	
5	SD-29		Pyr vein within # I-5 Ore Vein	422	n/a	406
6	SD-41		Pyr vein within # I-1 Ore Vein	420	n/a	(325-447)
7	SD-55		Pyr vein within # I-10 Ore Vein	444	145	
8	SD-65		Pyr vein within # I-8 Ore Vein	387	n/a	
9	SD-71		Pyr vein within # I Ore Zone	401	n/a	
10	SL-06	pyrite	from a QV outside the mine	207 (L)	n/a	
11	SL-10		from Permian metamorphosed basalt	n/a	n/a	
12	SD-17		from Pyr vein within III-2 Ore Vein	332 (E)	n/a	
13	SD-23		from #I-4 Ore Vein	396 (E)	n/a	366 (E)
14	SD-29		from #I-5 Ore Vein	362 (E)	n/a	(332-396)(E)
15	SD-41		from #I-1 Ore Vein	375 (E)	325	
16	SD-52		from a dolomite vein at schist-marble contact	234 (L)	131	
17	SD-55		from #I-10 Ore Vein	n/a	n/a	
18	SD-34	tetradymite	from #I-4 Ore Vein	231	78	
19	SD-36		from #I-5 Ore Vein	255	n/a	
20	SD-40		from #I-1 Ore Vein	222	n/a	229
21	SD-46		from #I-2 Ore Vein	223	n/a	(186-255)
22	SD-58		from #I-10 Ore Vein	248	n/a	
23	SD-59		from #I-10 Ore Vein	241	n/a	
24	SD-61		from #I-10 Ore Vein	186	n/a	
25	SL-23	chalcocite	from (No Suggestions) Cu-Au showing nearby	112, 181, 313	n/a	n/a
26	SD12-1	dolomite	from a dolomite vein between # II & III Ore Zones	298 (E)	n/a	
27	SD-23		from #I-4 Ore Vein	317 (E)	n/a	
28	SD-29		from #I-5 Ore Vein	301, 344 (E)	n/a	
29	SD-36		from #I-5 Ore Vein	308 (E)	n/a	317 (E)
30	SD-40		from #I-1 Ore Vein	334 (E)	n/a	(250-452)
31	SD-46		from #I-2 Ore Vein	317, 375 (E)	n/a	
32	SD-59		from #I-10 Ore Vein	334, 406 (E)	n/a	
33	SD65-1		from #I-8 Ore Vein	452, 250 (E)	169, 59	
34	SD-62		from #I-9 Ore Vein	155 (E)	n/a	159.5 (E)
35	SD-71		Pyr vein within # I-1 Ore Vein	164 (E)	n/a	(155-164)
36	SD-70		from a dolomite vein within #I Ore Zone	150 (L)	n/a	
37	SD-52		from a dolomite vein at schist-marble contact	298 (L)	n/a	241 (L)
38	SD-44		from #I-3 Ore Vein	267 (L)	320	(150-298)
39	SL-09		from a dolomite vein outside the mine	250 (L)	n/a	
40	SD-49	calcite	from the banded marble within the mine	327	n/a	287.5
41	SD-69		from coarse grained marble within the mine	248	n/a	(248-327)
42	SD-10	chalcopyrite	from a quartz vein between # II & III Ore Zones	346	n/a	
43	SD-15		from the Pyr vein of # III Ore Zone	298	n/a	336
44	SD-16		from the #III-2 Pyr vein	363	n/a	(298-363)
45	SD-71		from the Pyr vein within # I Ore Zone	n/a	435	
46	SD-11	quartz	from a quartz vein between # II & III Ore Zones	174, 399	n/a	117
47	SD-26		from #I-4 Ore Vein	100	n/a	(78-174)
48	SD-27		from #I-5 Ore Vein	78	n/a	
49	SL-11	tourmaline	from a tourmaline-quartz vein outside the mine	94	n/a	94

Note: E - the early metallogenic stage, L - the late metallogenic stage.

Table 2a : Characteristics of fluid inclusions in the minerals from the deposit.

series #	sample #	mineral	sample location		occurrence	fluid inclusion description
1	SL-06	quartz	periphery of the mine	beside a road to the west of the Dashuigou mine	from a white, yellowish brown QV with muscovite, Py, Pyr & Cp disseminations in a strata just above the Te-bearing stratohorizon	5-10μm, up to 20μm, oval, polygon or irregular gaseous-liquid inclusions, g/l ≥ 30%, some over 50%
2	SL-11	quartz		to the west of mine	from a broken white tourmaline-quartz vein in a strata just below the Te-bearing stratohorizon	5-10μm, up to 25μm, oval, irregular or polygon gaseous-liquid inclusions in groups, generally g/l > 50%
3	SD-09	quartz	within the mine	Ore Zone II	60cm thick milky white & yellowish brown quartz vein cross cutting the country rocks	5-10μm, some up to 30μm, scattered regular polygon, g/l > 50%, a few 3 phases
4	SD-11	quartz		QV between Ore Zone II and III	pure milky white quartz vein parallel to the tellurium veins	5-10μm, some up to 20μm, scattered irregular, g/l=5%-10%, a few 3 phases with perfect cubic NaCl crystals
5	SD12-1	quartz		QV between Ore Zone II and III	quartz-dolomite compound vein with muscovite	5-20μm, strip, tubular, or irregular, g/l=5%-10%, a few liquid & few 3 phases
6	SD-25	quartz		#I-4 Ore Vein	broken quartz vein with disseminated pyrite locally	3-10μm, up to 20-30μm, oval, polygon, irregular, g/l<50%, a few gaseous & few 3 phases
7	SD-26	quartz			at a sharp, straight and clear contact with the altered wall rocks	5-10μm, up to 20-30μm, oval or irregular, some polygon, generally g/l<50%
8	SD-27	quartz			quartz with fine pyrite & pyrrhotite veinlets locally	5-10μm, up to 45μm, oval, polygon, irregular, g/l<50%, a few inclusions' g/l>50%
9	SD-67	quartz		#I-7 Ore Vein	pure white quartz vein with muscovite and bismuth sulfide locally	5-10μm, up to 20μm, regular polygon, g/l=20%, a few gaseous & 3 phases with NaCl
10	SD-62	dolomite		#I-9 Ore Vein	very coarse grained dolomite with iron staining locally	3-10μm, regular polygon, not rich in dolomite, scattered, mainly liquid, g/l around 5%
11	SD65-1	dolomite		#I-8 Ore Vein	pure white, coarse-giant grained dolomite	3-5μm, oval, not very rich, scattered, mainly liquid, g/l is around 5%
12	SD-70	dolomite		dolomite vein within #IV Ore Zone	coarse-giant grained dolomite with a few pyrite and pyrrhotite disseminations	3-5μm, oval, very limited, scattered, mainly liquid, g/l is generally less than 5%
13	SD-69	calcite		coarse-grained marble beneath the Te-bearing stratohorizon	pure white and clean calcite	3-5μm, polygon, very rich, scattered, mainly liquid, g/l is generally below 5%

Notes: QV-quartz vein, Py-pyrite, Pyr-pyrrhotite, Cp-chalcopyrite, g/l-gas/liquid ratio within an inclusion.

To be cont'd

Fluid inclusions in both dolomite and calcite are usually oval and/or polygon in shape, while those in quartz are either oval, polygon, irregular, strip and/or tubular. A few perfect cubic NaCl crystals could be seen in several of the fluid inclusions in quartz (Figure 9).

Chemical Compositions

Chemical compositions of the fluid inclusions of part of the gangue and ore minerals are listed in Table 3. It can be seen from the table that cations in the fluid inclusions include Na^+, K^+, Ca^{2+} and Mg^{2+}, while anions include SO_4^{2-}, Cl^- and F^-, and the major gaseous compositions include H_2O and CO_2, with smaller CH_4, H_2, N_2, CO and C_2H_6. Na^+/K^+ ratios of the fluid inclusions of the region's minerals are either above or below 1.0, meaning that compositions of the hydrothermal solutions are not homogeneous. Ca^{2+}/ Mg^{2+} ratios of the fluid inclusions are

Table 2b : Characteristics of fluid inclusions in the minerals from the deposit (*cont'd*).

series #	3pIHT[1] (°C)	NCIVT[2]	DT[3]	HT[4]	salinity (wt.%)	pressure[5]	depth[6]
	$LCO_2+VCO_2 \rightarrow LCO_2$	°C	°C	°C	NaCl	Kbar	km
1	9.0	n/a	207.0 pyrite in quartz vein	291.3-419.4 369.4	10.4-17.6 13.8	1.950	7.80-6.50
2	21.3	n/a	94.0 tourmaline in QV	337.0-340.1 339.0	13.5-16.8 15.2	1.340	5.36-4.47
3	21.0	n/a	n/a	144.0-203.0 180.0	15.1-18.4 16.2	0.515	2.06-1.72
4	25.4	219.9-300.8	174.4	367.0-425.9 397.0	34.0-38.5 36.2	1.540	6.16-5.13
5	15.0	(188.0-234.6)* 219.3	n/a	403.8-426.8 415.3	18.4-34.6 26.6	1.800	7.20-6.00
6	13.4	n/a	n/a	209.8-234.0 225.0	15.2-21.3 18.7	1.020	4.08-3.40
7	22.4	n/a	100.0	173.0-251.0 216.3	15.6-21.3 18.0	0.882	3.53-2.94
8	19.0	n/a	78.0	148.0-252.3 202.3	12.0-18.6 14.9	0.647	2.59-2.16
9	21.9	195.6-330.0 258.8	n/a	195.5-522.4 337.7	15.0-40.5 27.4	0.956	3.82-3.19
10	n/a	n/a	155.0	165.0	n/a	n/a	n/a
11	n/a	n/a	169, 250, 452	238.0	n/a	n/a	n/a
12	n/a	n/a	150.0	134.7	n/a	n/a	n/a
13	n/a	n/a	248.0	147.4-213.9 180.7	0.5-5.6 3.1	n/a	n/a

Notes: 1 - 3-phase inclusion homogenization temperature, 2 - NaCl crystal inclusion vanished temperature, 3 - decrepitation temperature (see Table 1), 4 - homogenization temperature, 5 - calculated on isoline analysis, 6 - calculated at a pressure rate of (0.25 - 0.30) x 10^8 Pa/km (1bar = 1 x 10^5 Pa), (188.0-234.6)/219.3)* - (min value - max value)/average value.

all above 1.0, meaning that the metallogenic solutions are rich in Ca^{2+} but poor in Mg^{2+}. Both SO_4^{2-}/Cl^- and Cl^-/F^- ratios are over 1.0, meaning that the metallogenic solutions are richest in SO_4^{2-}, moderate in Cl^-, but poor in F^-. Most of the samples had H_2O/CO_2 ratios of over 1.0, meaning the solutions are richer in H_2O than in CO_2. $(CO_2 + H_2 + CH_4)/N_2$ values of all samples are over 1.0, showing that the hydrothermal solutions are rich in CO_2, H_2 and CH_4.

Discussion

Previous research on the ore-forming fluid of the Dashuigou tellurium deposit is roughly divided into the magma hydrothermal theory [4-6,10,11,26,28,29], the metamorphic hydrothermal theory [30,31], and the mixed hydrothermal theory [5,9,30] obtained the study of gas-liquid inclusions and found that the ore-forming temperature of the Dashuigou tellurium deposit varied between 350 and 120°C. The salinity is 7.2 wt% ~ 35 wt% NaCl, of which the salinity value in the early and late quartz veins can be as high as 20 wt% to 35 wt% NaCl, the oxygen fugacity is f_{O2} = -42.26 ~ -45.49, and the ore-forming hydrothermal fluid is weakly acidic and neutral (pH = 6.32 ~ 6.29). The CO_2/H_2O ratio in the quartz is 0.137 ~ 0.208, and the CH_4 content is 12.61 ~ 24.85 ml/100 g. Based on uniform temprature measurement of the gas-liquid inclusions in the deposit's dolomite and quartz, Li [29] and Cao [10-11] concluded that the uniform temperature of each mineralization stage is roughly similar: 221 ~ 259°C, average 239°C for Stage I; 215 ~ 256°C, average 235°C for Stage II; 192 ~ 243°C, average 224°C for Stage III. The corresponding metallogenic pressure is 823.684 × 10^5 Pa ~ 965.409 × 10^5 Pa, with an average of 884.156 × 10^5 Pa. Both CO_2 and H_2O-CO_2 inclusions are abundant, reflecting that mineralization occurs under relatively closed conditions. The metallogenic depth estimated by the static rock pressure model is 3,339 m, which is equivalent to the thickness of the measured overlying strata (3650 m). Since the characteristics of inclusion types in each mineralization stage are not substantially different, they are considered to have similar metallogenic depths.

Table 3a : Chemical compositions of the gaseous-liquid fluid inclusions in the minerals.

series #	sample #	mineral	sample location	gaseous composition (μg/g)						
				H_2O	CO_2	H_2	CH_4	N_2	CO	C_2H_6
1	SD-11	quartz	QV between #II & III Ore Veins	246.0	200.0	0.120	1.600	5.500	0.001	0.001
2	SD-26	quartz	from #I-4 Ore Vein	366.0	236.0	0.105	11.700	2.000	0.001	0.001
3	SD-27	quartz	from #I-4 Ore Vein	150.0	160.0	0.018	10.000	1.800	0.001	0.001
4	SL-11	tourmaline	from a QV outside the mine	117.0	342.0	0.150	4.000	1.300	0.001	0.001
5	SL-09	dolomite	from a DV outside the mine	210.0	164.0	2.640	2.600	0.800	0.001	0.001
6	SD12-1	dolomite	a DV between #II & III Ore Veins	334.0	640.0	4.750	1.600	1.800	0.001	0.001
7	SD-40	dolomite	from #I-1 Ore Vein	150.0	1136.0	5.340	5.200	3.250	0.001	0.001
8	SD-44	dolomite	from #I-3 Ore Vein	700.0	828.0	22.200	2.000	18.000	0.001	0.001
9	SD-46	dolomite	from #I-2 Ore Vein	282.0	3500.0	3.100	14.000	5.000	0.001	0.001
10	SD-59	dolomite	from #I-10 Ore Vein	162.0	828.0	10.600	3.400	4.000	0.001	0.001
11	SD-62	dolomite	from #I-9 Ore Vein	282.0	904.0	4.480	2.000	5.750	0.001	0.001
12	SD65-1	dolomite	from #I-8 Ore Vein	282.0	945.0	4.000	4.440	10.500	0.001	0.001
13	SD-71	dolomite	from Pr-D vein of #IV ore zone	210.0	1250.0	4.990	12.400	4.000	0.001	0.001
14	SD-49	calcite	from banded marble at #4 adit portal	33.0	29.0	2.110	3.400	1.300	0.001	0.001
15	SD-69	calcite	from the Triassic marble of the mine	138.0	84.0	2.700	3.100	1.000	0.001	0.001
16	SD-10	pyrrhotite	from a Pyr vein between #II & III Ore Zones	812.0	224.0	0.075	0.001	2.250	0.001	0.001
17	SD-15	pyrrhotite	from #III-1 Pyr Vein	925.0	232.0	0.090	0.001	1.600	0.001	0.001
18	SD-55	pyrrhotite	from #I-10 Ore Vein	756.0	132.0	0.080	0.001	1.300	0.001	0.001
19	SD-65	pyrrhotite	from #I-8 Ore Vein	850.0	284.0	0.220	0.001	1.600	0.001	0.001
20	SD-41	pyrite	from #I-1 Ore Vein	15.0	10.0	0.001	0.001	1.300	0.001	0.001
21	SD-17	pyrite	from #III-2 Pyr Vein	21.0	18.0	0.001	0.001	1.600	0.001	0.001
22	SD-23	pyrite	from #I-4 Ore Vein	21.0	12.0	0.001	0.001	0.800	0.001	0.001
23	SD-29	pyrite	from #I-5 Ore Vein	27.0	20.0	0.001	0.001	1.000	0.001	0.001
24	SD-55	pyrite	from #I-10 Ore Vein	21.0	18.0	0.001	0.001	0.000	0.001	0.001
25	SD-15	chalcopyrite	from #III-1 Pyr Vein	344.0	58.5	0.018	0.001	1.000	0.001	0.001

Note: DV - dolomite vein, Pyr - D-pyrrhotite-dolomite.

to be continued

According to the ore-forming pressure and salinity, the temperature correction value was found to be about 80°C, so the metallogenic temperatures of stages I, II, and III were 319°C, 315°C, and 304°C, respectively. The salinity of ores from this deposit varies widely, with NaCl content ranging from 7.17% to 33.27%. Among them, the rock salt gas-liquid water inclusions have the highest salinity, while the gas-liquid water inclusions and liquid-liquid H_2O-CO_2 inclusions have lower salinity and are basically the same. The salinity of fluids in each mineralization stage is roughly similar, where the NaCl content in stage I is 16.5% ~ 30.83%, with an average of 21.21%; stage II is 17.66% ~ 33.27%, with an average of 25.77%; stage III is 7.17% ~ 32.34%, with an average of 17.55%. The gas phase composition is mainly H_2O, followed by CO_2, and containing a small amount of H_2, CO and CH_4. According to observation under a microscope, the fluid inclusions in the minerals from this deposit are mainly H_2O-CO_2 and CO_2. The f_{O2} of the mineralization fluid is: stage I 10.0×10^5 ~ 34.0×10^5 Pa, stage II 10.0×10^5 ~ 34.8×10^5 Pa, stage III 10.0×10^5 ~ 35.6×10^5 Pa. The pH value of the hydrothermal solution during the tellurium mineralization stage is 5.91 ~ 5.87. Through study of gas-liquid inclusions from the same deposit, Chen [28] concluded that the inclusions are rich in CO_2, CO_2-H_2O (low salinity fluid), and CO_2-H_2O-NaCl (high salinity fluid); namely, three systems of fluid inclusions exist in the deposit, of which tellurium mineralization is related to the first two systems. Most of the inclusions leak and/or burst before being homogenized. The metallogenic temperature of the pyrrhotite stage is around 500°C and that of the telluride stage is 400°C. The fluid density changes between 1.04 ~ 0.76 g/cm^3, and the metallogenic pressures are respectively 450 ~ 500 MPa and 240 ~ 300 MPa. Mineralization occurs under high temperature and high pressure. The results of this paper are as follows: fluid inclusion homogenization temperatures vary greatly (Table 2): those of quartz formed in pre-tellurium mineralization and collected outside the deposit are between 339.0 and 369.4°C. These samples include series #1, 2, 4 and 5 in Table 2. Other quartz samples in Table 2 are associated with telluride veins and their fluid inclusion homogenization temperatures should be at typical values when tellurium ore bodies emplaced, or between 180.0-250.0°C. This range includes part of the decrepitation temperatures of those minerals formed during the tellurium epoch mentioned earlier in this paper. The salinity of fluid inclusions within the whole metallogenic epochs varies between 13.8%-36.2%, which falls into a medium-high salinity range. That of minerals formed during the tellurium epoch, for instance three quartz samples associated with tellurides and collected from #I-4 Ore Vein in Table 2, is between 14.9%-18.7%, well within the medium salinity range. The formation pressures of mineral fluid inclusions

Table 3b : Chemical compositions of the fluid inclusions in the minerals (*cont'd*).

series #	liquid composition (μg/g)									
	Na^+	K^+	Ca^{2+}	Mg^{2+}	Cl^-	F^-	SO_4^{2-}	NO_3^-	Br^-	PO_4^{3-}
1	22.90	8.20	1.8	1.14	8.01	1.19	43.8	0.00	0.00	0.00
2	15.10	6.56	1.5	0.98	4.68	1.10	39.5	0.00	0.00	0.00
3	11.40	5.45	1.2	0.33	2.21	0.91	49.5	0.00	0.00	0.00
4	7.81	4.92	1.8	2.45	1.51	1.41	32.6	0.00	0.00	0.00
5	2.92	2.18	n/a	n/a	4.02	0.40	50.7	0.00	0.00	0.00
6	13.30	3.27	n/a	n/a	26.30	0.95	70.4	0.00	0.00	0.00
7	4.88	2.46	n/a	n/a	11.40	1.60	100.0	0.00	0.00	0.00
8	4.22	4.36	n/a	n/a	8.83	1.80	187.0	0.00	0.00	0.00
9	2.60	0.001	n/a	n/a	25.50	13.80	5490.0	0.00	0.00	0.00
10	19.50	32.80	n/a	n/a	4.58	3.78	1934.0	0.00	0.00	0.00
11	10.10	7.08	n/a	n/a	11.30	0.87	471.0	0.00	0.00	0.00
12	8.30	2.46	n/a	n/a	1.82	0.44	225.0	0.00	0.00	0.00
13	6.82	3.27	n/a	n/a	6.69	1.60	1313.0	0.00	0.00	0.00
14	2.44	2.46	n/a	n/a	4.84	0.62	147.0	0.00	0.00	0.00
15	1.95	3.28	n/a	n/a	2.34	0.97	49.7	0.00	0.00	0.00
16	63.40	82.00	1000.0	909.0	1.40	0.97	n/a	0.00	0.00	0.00
17	29.30	24.60	1750.0	2545.0	2.08	1.98	n/a	0.00	0.00	0.00
18	29.30	24.60	750.0	364.0	8.50	1.54	n/a	0.00	0.00	0.00
19	29.30	65.80	7500.0	273.0	1.98	1.76	n/a	0.00	0.00	0.00
20	12.20	16.40	1250.0	909.0	3.60	1.85	n/a	0.00	0.00	0.00
21	19.50	16.40	500.0	364.0	3.10	1.62	n/a	0.00	0.00	0.00
22	22.00	8.20	1500.0	182.0	1.44	1.85	n/a	0.00	0.00	0.00
23	14.60	16.40	1250.0	273.0	5.70	4.62	n/a	0.00	0.00	0.00
24	34.20	49.20	500.0	454.0	3.80	2.23	n/a	0.00	0.00	0.00
25	39.00	32.80	1750.0	1091.0	1.77	1.32	n/a	0.00	0.00	0.00

to be continued

Table 3c : Chemical compositions of the fluid inclusions in the minerals (*cont'd*).

series #	Na^+/K^+	Ca^{2+}/Mg^{2+}	Cl^-/F^-	SO_4^{2-}/Cl^-	H_2O/CO_2	$(CO_2+H_2+CH_4)/N_2$
1	2.79	1.58	6.73	5.47	1.230	36.680
2	2.30	1.53	4.25	8.44	1.550	123.900
3	2.09	3.64	2.42	22.40	0.940	94.450
4	1.59	0.73	1.07	21.60	0.340	266.270
5	1.34	n/a	10.18	12.61	1.280	211.550
6	4.07	n/a	27.83	2.67	0.520	359.080
7	1.98	n/a	7.13	8.77	0.130	365.910
8	0.95	n/a	4.91	21.18	0.850	46.410
9	2600.0	n/a	1.85	215.29	0.080	707.240
10	0.59	n/a	1.21	422.27	0.200	208.630
11	1.43	n/a	12.99	41.68	0.310	159.410
12	3.37	n/a	4.14	123.63	0.300	90.850
13	2.09	n/a	4.18	196.26	0.170	316.850
14	0.99	n/a	7.86	30.37	1.140	26.550
15	0.59	n/a	2.42	21.24	1.640	89.800
16	0.77	1.10	1.45	n/a	3.630	99.590
17	1.19	0.69	1.05	n/a	3.990	145.060
18	1.19	2.06	5.52	n/a	5.730	101.600
19	0.45	27.47	1.13	n/a	2.990	177.640
20	0.74	1.38	1.95	n/a	1.500	7.690
21	1.19	1.37	1.91	n/a	1.170	11.250
22	2.68	8.24	1.32	n/a	1.750	15.000
23	0.89	4.58	1.23	n/a	1.350	20.002
24	0.70	1.10	1.70	n/a	1.170	∞+
25	1.19	1.60	1.34	n/a	5.880	58.519

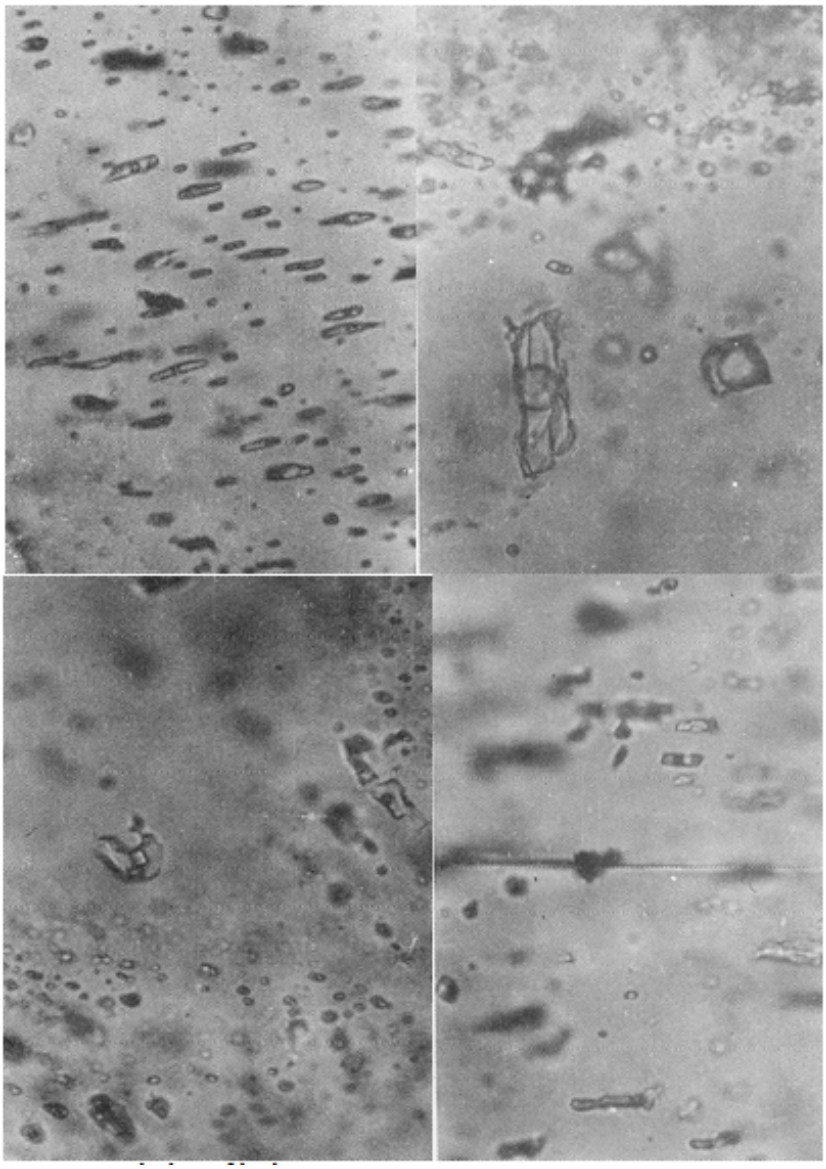

Figure 9: Fluid inclusions in quartz and calcite of the deposit. A: gaseous-liquid inclusions in quartz from #I-4 Ore Body (X 400), B: gaseous inclusions in quartz from #I-4 Ore Body (X 400), C: cubic NaCl crystal in gaseous-liquid inclusions in quartz from #I-7 Ore Body (X 400), D: gaseous-liquid inclusions in calcite from coarse grained marble of the lower Triassic strata of the deposit (X 400).

correlate positively with homogenization temperatures (Table 2). Pressures of the series #6 through #9 samples in the table, acquired from minerals formed during tellurium mineralization, vary between 0.647-1.02 Kbar. This should be the pressure at which point telluride veins emplaced in the deposit. The corresponding mineralization depth is 4.08-2.16 km, while mineralization temperatures of the early and late metallogenic epochs of the deposit are respectively 336.0-406.0 and 216.9-229.0°C. Fluid inclusion compositions in both pyrrhotite and pyrite that formed in the same mineralization stage of the metallogenic epoch are similar to each other. Those of fluid inclusions in quartz samples collected from the deposit are also alike. Compositions of fluid inclusions of dolomite and calcite have both similarities and differences, especially those of dolomite and calcite collected from outside the deposit compared to those collected within the deposit. Differences also exist between dolomite from wall-rock marble and from dolomite veins. This may mean that compositions of fluid inclusions vary from one host mineral to another, and minerals formed in different environments or across different geological events have different fluid inclusion compositions. The metallogenic hydrothermal solutions, which are not homogeneous, are richest in SO_4^{2-}, richer in H_2O than in CO_2, rich in Ca^{2+}, CO_2, H_2, and CH_4, moderate in Cl^-, but poor in Mg^{2+} and F^-.

Conclusion

Based on the discussions above, preliminary conclusions of the Dashuigou independent tellurium mine's metallogenic conditions are summarized as follows: The metallogenic hydrothermal solutions are SO_4^{2-} - Ca^{2+} type, or SO_4^{2-} - Na^+ - K^+ - Ca^{2+} type, especially during the early metallogenic Pyritic Epoch, and Na^+ - K^+ - Cl^- SO_4^{2-} type during the late metallogenic epoch. The hydrothermal

solutions of the deposit are mesothermal and of moderate salinity, as well as mesogenetic. Principal compositions of the metallogenic hydrothermal fluids are Na+, K+, - Ca^{2+}, Mg^{2+}, SO_4^{2-}, Cl^-, F H_2O, CO_2, CH_4, H_2, N_2, CO and C_2H_6; Salinity of the fluid inclusions within the metallogenic epochs varies between 13.8%-36.2%, which falls into the medium-high salinity range; that of minerals formed during tellurium epoch, for instance, three quartz samples associated with tellurides and collected from #I-4 Ore Vein in Table 2, is 14.9%-18.7%, which is within the medium salinity range. Metallogenic pressure is between 0.647-1.020 Kbar and the corresponding mineralization depth is 4.08-2.16 km. Mineralization temperatures of the early and late metallogenic epochs of the deposit are respectively 336.0-406.0 and 216.9-229.0°C.

Acknowledgement

Support for this study was received from the China National Postdoctoral Foundation, Orient Resources Ltd., and Bureau Veritas Commodities Canada Ltd. Additional support was provided respectively by Prof. R. Pei of the Chinese Academy of Geological Sciences, also an Academician of the Chinese Academy of Engineering, Prof. Y. Zhai of China University of Geosciences in Beijing, also an Academician of the Chinese Academy of Sciences, Prof. J. Zhou of the Chinese Academy of Geological Sciences, and Prof. Y. Zhang of the College of Earth Sciences, Jilin University in Changchun of China, all of whom provided insightful discussions and critical reviews of this manuscript. All measurements and chemical analyses, including the back scattered electron (composition) and Te Kα X ray images of the thin section from the deposit, included in this article were carried out in the labs of the Chinese Academy of Geological Sciences in Beijing. The authors very much appreciate the time invested respectively by D. S. Yin and S. Daly, for their review and editorial work on this contribution.

Data Availability

The data that support the findings of this study is available from the authors upon reasonable request; see authors' contributions for specific data sets below.

Contributions

The whole research included in the paper was proposed and done by the first author J. Yin. The chemical compositions of fluid inclusions were sorted and researched by the second author Hongyun Shi of this paper. Both authors prepared and reviewed the manuscript and approved the final version of the manuscript. Author Contributions. Conceptualization, JIANZHAO YIN; Investigation, JIANZHAO YIN and Hongyun Shi; Project administration, JIANZHAO YIN; Writing – original draft, JIANZHAO YIN.

Competing Interests

The authors declare no competing interests.

References

1. Li T (1976) Abundance of chemical elements in the Earth. *Geochemistry* 3: 167-174.
2. Yin, JZ, Chen, YC, Zhou, JX (1995) Introduction of tellurium resources in the world. *Journal of Hebei College of Geology* 18: 348-354.
3. Yin, JZ (1996) On the metallogenic model and mineralizing mechanism of the Dashuigou independent tellurium deposit in Shimian County, Sichuan Province, China-the first and only independent tellurium deposit in the world. Chongqing: Chongqing Publishing House, 190pp.
4. Chen YC, Mao JW, Luo YN, Wei JX, Cao, ZM. (1996) Geology and Geochemistry of the Dashuigou tellurium (gold) deposit in Western Sichuan, China. *Beijing: Atomic Energy Press* 146pp.
5. Luo, YN, Fu DM, Zhou, SD (1994) Genesis of the Dashuigou tellurium deposit in Sichuan Province of China. *Bulletin of Sichuan Geology* 14: 101-110.
6. Luo YN, Cao ZM, Wen, CQ (1996) Geology of the Dashuigou independent tellurium deposit. Chengdu: Southwest Communication University Publishing House 30-45.
7. Yin JZ (1996) The metallogenic model and mineralizing mechanism of the Dashuigou independent tellurium deposit in Shimian County, Sichuan - the first and only independent tellurium deposit in the world. *Acta Geoscientia Sinica* special issue 93-97.
8. Yin JZ, Shi HY (2019) Nano effect mineralization of rare elements--taking the Dashuigou tellurium deposit, Tibet Plateau, Southwest China as the example. *Academia Journal of Scientific Research* 7: 635-642.
9. Wang RC, Lu, JJ, Chen XM (2000) Genesis of the Dashuigou tellurium deposit in Sichuan Province, China. *Bulletin of Mineralogy, Petrology and Geochemistry* 4: 348~349.
10. Cao ZM, Luo YN (1994) Mineral sequence and ore genesis of the Sichuan telluride lode deposit in China. In: New Research Progresses of the Mineralogy, Petrology and Geochemistry in China. Lanzhou: Lanzhou *University Publishing House* pg: 476-478.
11. Cao ZM, Wen CQ, Li BH (1995) Genesis of the Dashuigou tellurium deposit in Sichuan Province of China. *Science China (B)* 25: 647-654.
12. Yin, JZ, Zhou JX, Yang BC (1994) Geological characteristics of the Dashuigou tellurium deposit in Sichuan Province, China. *Earth Science Frontiers* 1: 241-243.
13. Yin, JZ, Chen, YC and Zhou, JX (1995) Original rock of the host rock of the Dashuigou independent tellurium deposit in Sichuan Province, China. *Bulletin of Mineralogy, Petrology and Geochemistry* 2: 114-115.
14. Yin JZ, Chen YC, Zhou JX (1996) Geology and geochemistry of host rocks of the Dashuigou independent tellurium deposit in Sichuan Province, China. *Journal of Changchun University of Earth Sciences* 26: 322-326.
15. Yin JZ, Chen YC, Zhou JX (1996) Geology and geochemistry of altered rocks of the Dashuigou independent tellurium deposit in Sichuan Province, China. *Journal of Xi'an College of Geology*, 18: 19-25.
16. Chen YC, Yin JZ, Zhou JX (1994) The first and only independent tellurium ore deposit in Dashuigou, Shimian County, Sichuan Province, China. *Sci. Geol. Sinica* 3: 109-113.
17. Chen YC, Yin JZ, Zhou, JX (1994) Geology of the Dashuigou independent tellurium deposit of Sichuan Province. *Acta Geoscientia Sinica* 29: 165-167.
18. Yin JZ, Zhou JX, Yang BC (1994) Rock-forming minerals and ore-forming minerals of the Dashuigou tellurium ore deposit unique in the world - A preliminary study. *Sci. Geol. Sinica* 3: 197-210.
19. Yin, JZ, Chen YC, Zhou JX (1994k) Mineralogical research of the Dashuigou independent tellurium deposit in Sichuan Province, China. *Bulletin of Mineralogy, Petrology and Geochemistry* 3: 153-155.
20. Yin JZ (1996) New mineralogical data of telluride. *Bulletin of Mineralogy, Petrology and Geochemistry* 15: 246-248.
21. Liu AP, Zhong ZC, Tang JW (1996) Geochemical characteristics of the Dashuigou tellurium deposit in Sichuan Province of China. *Geochemistry* 25: 365~371.
22. Shi HY, Chen YC, Yin JZ, Zhou JX (1996) X-ray diffraction data of telluride. *Journal of Mineralogy and Petrology* 16: 31-33.
23. Yin JZ, Shi HY (2020) Mineralogy and stable isotopes of tetradymite from the Dashuigou tellurium deposit, Tibet Plateau, southwest China. *Scientific Reports* 10.
24. Yin JZ, Chen YC, Zhou JX (1995) K-Ar isotope evidence for age of the first and only independent tellurium deposit. *Chinese Science Bulletin* 40**:** 1933-1934.
25. Li BH, Cao ZM, Wen CQ (2000) Fluid inclusion type and geological characteristics of the Dashuigou tellurium deposit in Sichuan Province, China. *Bulletin of Mineralogy, Petrology and Geochemistry* 4: 346-347.

26. Li TY, Liu JQ (2000) Discussion of analytical methods of grouped fluid inclusion compositions. *Geology and Mineral Resources of South China* 4: 64-67.

27. Li BL (1986) Physical chemistry diagram of gas components of fluid inclusions in minerals. *Geochemistry* 2: 126-137.

28. Chen PR, Lu JJ, Wang RC (1998) Study on the fluid inclusions of the Dashuigou independent tellurium deposit in Shimian County, Sichuan Province, China. *Mineral Deposit* 17: 1011-1014.

29. Li BH, Cao ZM, Jin JF, Wen CQ (1999) Physicochemical conditions of the tellurium deposit in Dashuigou, China. *Scientia Geologica Sinica* 34: 463-472.

30. Wang RC, Shen WZ, Xu XJ, Lu JJ, Chen XM, et al. (1995) Isotopic Geology of the Dashuigou tellurium deposit in Sichuan Province, China. *Journal of Nanjing University (Natural Sciences)* 31: 617-624.

31. Shen WZ, Xu XJ, Wang RC (1997) Origin of the fluid inclusions of the Dashuigou tellurium deposit in Sichuan Province, China - hydrogen and oxygen isotope evidence. *Journal of Nanjing University (Natural Sciences)* 33: 77-83.

Citation:

Yin J, Shi H (2021) Fluid Inclusions and Metallogenic Conditions of the Dashuigou Tellurium Deposit, Tibet Plateau, Southwest China. *Geol Earth Mar Sci* Volume 3(3): 1-15.